Journal of Power Sources 620 (2024) 235094

Contents lists available at ScienceDirect

Journal of Power Sources

journal homepage: www.elsevier.com/locate/jpowsour

Time delay in the charge/discharge of fractional-order capacitive energy storage devices

Enrique H. Balaguera [a,b,*], Anis Allagui [b]

[a] Escuela Superior de Ciencias Experimentales y Tecnología, Universidad Rey Juan Carlos, C/ Tulipán, s/n, 28933, Móstoles, Madrid, Spain
[b] Department of Sustainable and Renewable Energy Engineering, University of Sharjah, PO Box 27272, Sharjah, United Arab Emirates

HIGHLIGHTS

- Steady-state analysis of the fractional-order capacitor.
- Concept of "incremental capacitance" in the transition from C to CPE.
- Charge/discharge time depends strongly on the dispersive exponent.
- Experimental study of supercapacitors using the theory proposed.

ARTICLE INFO

Keywords:
Capacitance
Constant phase element
Transient analysis
Fractional calculus
Steady-state response
Supercapacitor

ABSTRACT

Electrical energy storage devices exhibit dispersive properties that control their charge and discharge processes. To get a deeper understanding of these anomalous phenomena, it is essential to go beyond static viewpoints of circuit theory in order to accurately characterize the complex interplay of internal mechanisms. Specifically, the (dis)charging time of resistive-capacitive networks is commonly estimated as four times the product of the Thévenin resistance and the capacitance itself by assuming ideal exponential relaxations in spite of the intrinsic fractional dynamics of the real energy storage materials, leading to inaccurate and erroneous characterization protocols. The purpose of this work is to provide recommended practices to find the steady-state operation of such type of devices from time-domain data with a decelerated behavior of the Mittag-Leffler function at long time scales, introducing the concept of "incremental capacitance" in the transition from ideal to fractional-order capacitor and thus, an estimation of the charge/discharge time delay. Our theoretical analysis is validated by providing a representative example of experimental application, based on an electrochemical power source, such as supercapacitors under switching-type operation. We hope to bring such study to the attention of multidisciplinary readers, both from academia and industry, focused on energy storage device research.

1. Introduction

Conceptually, the electrical traces that describe the physics-based internal phenomenology of the vast majority of energy storage devices consist of resistive and capacitive features [1]. From the point of view of network analysis, the key component here is the capacitor (C) [2] which provides the relaxation dynamics attributable to the charging and discharging processes of such electrical model due to the current $i_C(t)$ is proportional to the rate at which the voltage $v_C(t)$ across the capacitor varies with time [3],

$$i_C(t) = C\frac{dv_C(t)}{dt} \tag{1}$$

where $i_C(t)$ is measured in amperes, C in farads, $v_C(t)$ in volts, and t in seconds. We remind that Eq. (1) is obtained from the general theory of the Maxwell's equations, $q_C(t) = Cv_C(t)$, relating the charge $q_C(t)$ and the voltage in a linear time-invariant (LTI) capacitor [4].

One of the most widely experiments to electrically characterize LTI materials is Impedance Spectroscopy (IS) [5], that quantifies the opposition exhibited by the sample under test to the flow of alternating current over a frequency range of interest. In Nyquist plots, the theoretical spectral picture of a capacitor shows a straight line forming an

* Corresponding author. Escuela Superior de Ciencias Experimentales y Tecnología, Universidad Rey Juan Carlos, C/ Tulipán, s/n, 28933, Móstoles, Madrid, Spain.
E-mail address: enrique.hernandez@urjc.es (E. H. Balaguera).

https://doi.org/10.1016/j.jpowsour.2024.235094
Received 21 March 2024; Received in revised form 10 June 2024; Accepted 21 July 2024
Available online 21 August 2024

angle of $-\pi/2$, leading to the famous diagrams that consist of impedance arcs underlying natural processes with resistive and capacitive features [6]. The dielectric properties are theoretically described by the impedance function of the capacitor, $Z_C(\omega) = {}^{1}/_{j\omega C}$, where j is the imaginary number and ω is the angular frequency. In time domain, the relaxation responses for basic step experiments, on the other hand, should be conceptually described in terms of decaying exponential functions with time [7] as result of the following evolution equation of the voltage across the "internal capacitance" of the resulting electrical models:

$$\frac{dv_C(t)}{dt} + \frac{v_C(t)}{\tau} = K \tag{2}$$

where τ is a positive constant representing a single characteristic relaxation time and, in effect, the exponential transient term $e^{-t/\tau}$ arises as the eigenfunction of the homogeneous version of Eq. (2), with $K = 0$ [8]. Note that K in Eq. (2) has the units of ${}^{V}/_{s}$. Any dynamical system is characterized, in part, by the value of its time constant τ. In circuit theory, τ is the reciprocal of the characteristic frequency (with changed sign) of the impedance or admittance, depending on if one considers current- or voltage-controlled operation [9,10], determining the rate at which the exponential term approaches zero. Without loss of generality, the time constant for electrical circuits with resistive-capacitive properties equals the product of the Thévenin resistance and capacitance [3,11], denoted as:

$$\tau = R_{Th}C \tag{3}$$

where the value of R_{Th} corresponds to the resistance "seen" from the terminals of the capacitor, differing if the independent input is a current or a voltage (deactivated for this purpose as open- and short-circuits, respectively). Apart from the free or natural transient component associated exclusively to the morphology of the circuit, the analytical response can also present a forced term which, in the case of a constant stimulus of duration T under study here, corresponds to the steady-state solution due to $dv_C(t)/dt\big|_{t\to\infty} = 0$ when $v_C(t)$ reaches its final value (mathematically expressed as $v_C(\infty)$) [8]. In fact, the forced response thus depends on both the electrical circuit and the excitation and thus,

$$v_C(\infty) = K\tau \tag{4}$$

Differential equations theory shows that, rearranging terms in Eq. (2) and integrating by using $t = 0$ and $v_C(0) = 0$ V (initial discharge state in the capacitor) as lower limits and t and $v_C(t)$ as upper limits,

$$\frac{dv_C(t)}{v_C(t) - v_C(\infty)} = -\frac{dt}{\tau} \rightarrow \int_0^{v_C(t)} \frac{dv_C(t)}{v_C(t) - v_C(\infty)} = -\frac{1}{\tau}\int_0^t dt \tag{5}$$

the complete solution for $v_C(t)$ emerges as [3,8]:

$$v_C(t) = v_C(\infty)\left(1 - e^{-t/\tau}\right), \quad 0 < t < T \tag{6}$$

which indicates that the voltage across the capacitor is zero before ($t = 0^-$) and just after the abrupt change ($t = 0^+$) in the driving excitation (continuity property, $v_C(0^-) = v_C(0^+)$ here [4]) and then increases exponentially to the steady-state value. At the instant of time in which the momentary transient event in terms of the exponential term in Eq. (6) can be considered negligible ($1 \gg e^{-t/\tau}$), the stored energy in the capacitor will be maximum ($v_C(t) \sim v_C(\infty)$). By inspection, it can be easily determined that, when the elapsed time from $t = 0$ exceeds three to five time constants, the dynamic route of $v_C(t)$ is triggered from the initial discharge to the new equilibrium state, practically attaining the steady-state level because the voltage response in the capacitor does not differ from $v_C(\infty)$ by more than ±5% ($e^{-3} \sim 0.05$) to ±1% ($e^{-5} \sim 0.007$), respectively [3]. Let's select

$$t_{ss,C} = 4\tau \tag{7}$$

as an intermediate value that represents the optimal solution (both efficacious and safe) [12]. At $t = 4\tau$, the voltage given by Eq. (6) reaches 98.2% of the final value, thus remaining within 2% of the expected final value. It is important to point out that the steady state is reached, mathematically speaking, only after an infinite hold time. In practice, however, a reasonable estimate of $t_{ss,C}$ is the length of time the response curve needs to go from 0 to approximately 98% of $v_C(\infty)$ here; that is, four time constants. Note that the above equations are also valid for an eventual discharge phase if the stimulus is switched off at time $t = T$. In this case, the transient response would show an exponential decay, rather that rise, with an initial value of $v_C(T)$ [11], yielding

$$v_C(t) = v_C(T)e^{-t/\tau}, \quad t > T \tag{8}$$

since the steady-state value would be zero now, $v_C(\infty) = 0$ V ($K = 0$ in Eq. (2)). Regarding the initial part, $v_C(T) = v_C(\infty)$ for $0 < t < T$ if the steady-state regime was reached in the charge phase ($T \geq t_{ss,C}$). Otherwise, $v_C(T) < v_C(\infty)$. Note that $v_C(t)$ is again a continuous function in the open interval (T^-, T^+) due to $i_C(t)$ would always remain bounded on this time range [3,4], unless the external stimuli exhibited an abrupt discontinuity (e.g., of impulsive nature) [8]. In any case, this ulterior post-excitation decay involves the same time constant as the charge process (see Eq. (6)), reaching again, in a practical purpose, its final value four time constants (Eq. (7)) after switching.

However, it is evident from many experimental data in the literature [13–15] that the dielectric relaxation responses in energy storage materials cannot be predicted from the simple capacitor theory. Rather, real-world physical processes with kinetics influenced by complexity or spatial heterogeneity generate non-Debye patterns [16], requiring a radical departure from the established paradigms. One of the most famous anomalous traces of the electrical responses in general are the depressed semicircle shapes in impedance responses [7,17]. However, this problem is classically circumvented by using the familiar constant phase element (CPE), with impedance $Z_{CPE}(\omega) = {}^{1}/_{Q(j\omega)^{\alpha}}$, in the fitting procedure [18] to an electrical model whose parameters are correlated with physical events of the material under study. In the modeling of spectral responses, CPE is invoked as a fractional-order capacitor [19] to account the non-ideal behavior of these complex materials, where $(j\omega)^{\alpha} = \omega^{\alpha}\angle\alpha\pi/2$, Q is a pseudocapacitive parameter in units of $F/s^{1-\alpha}$ and α is the dispersion coefficient ($0 < \alpha \leq 1$) that quantifies the deviation from the ideal capacitor ($\alpha = 1$). Different approaches in frequency-domain studies consider that this hybridized version of a resistor and a capacitor is a mathematical expression that models time-constant distributions along a surface [20] or through a film or layer [21] at microscopical level. Experimentally, analyzing the capacitive response of natural systems from the perspective of time-domain measurements also involves anomalies in terms of non-exponential or power-law profiles [22,23]. From a theoretical perspective, $(j\omega)^{\alpha}$ is indeed equivalent to the non-integer order derivative ${}^{d^{\alpha}}/_{dt^{\alpha}}$, which makes relaxation processes to go beyond the exponential dynamics [24]. In response to constant stimulus, closed forms based on the theory of fractional calculus have been already derived in the literature [25–27]. Specifically, there exists a range of published time-resolved procedures that explain the voltage relaxation dynamics, based on diffusion-controlled charge redistribution phenomena, in electrochemical power sources exhibiting non-ideal capacitive behavior. From different equivalent circuit models containing either one [13,28] or several CPEs [15,29] or even transmission lines [30,31] (equivalent in some way to such a dispersive element), many authors have obtained the corresponding analytical responses in the time domain describing the complex transient dynamics. In this sense, distribution of relaxation time (DRT) analyses has been also carried out during the last few years to study the dynamic behavior of real-world energy storage systems in a

coherent way under varying circumstances [32,33], visualizing especially the fast and slow charge phenomenology. However, the problem arises in any case because the fractional dynamics exhibits a characteristic pattern based on a long-time tail that leads to a time delay in the charge/discharge of most electrochemical power sources. To the authors' best knowledge, this has not been investigated yet, which we believe is important to provide a better understanding of the operational capabilities of this type of non-ideal energy capacitive storage devices.

In this paper, we provide a quantification of the time delay $\Delta t(\alpha)$ in the establishment of certain values of voltage across the dispersive capacitance using pseudo-steady-state analysis under constant excitations. This aspect is particularly important to estimate a differential capacitance obtained in the transition from ideal to fractional-order capacitor. We especially focus our attention on the impact of the fractionary exponent α on $\Delta t(\alpha)$. In the experimental section, we validate our theoretical analysis with charge/discharge cycles of voltages and currents obtained for the case of a source of electrochemical power, such as supercapacitors. The results provided here are essential for the optimization of analytical and experimental methods based on the processes of charge and discharge of capacitive systems, being of transversal application to several research fields.

2. Theoretical analysis

In the time domain, the corresponding current-voltage ($i_Q(t)$-$v_Q(t)$) relationship of the dispersive capacitance is represented by the fractional-order differential equation [19]:

$$i_Q(t) = Q\frac{d^\alpha v_Q(t)}{dt^\alpha} \tag{9}$$

Thus, Eqs. (2) and (3) can be rewritten as:

$$\frac{d^\alpha v_Q(t)}{dt^\alpha} = -\frac{v_Q(t) - v_Q(\infty)}{\tau^\alpha} \tag{10}$$

$$\tau = (R_{Th}Q)^{1/\alpha} \tag{11}$$

where $v_Q(\infty)$ represents the voltage across the fractional-order capacitor at long time scales and the value of τ in Eq. (11) denotes the characteristic time constant of the peak obtained in the DRT [34,35] of a R-CPE structure. The operator $d^\alpha v_Q(t)/dt^\alpha$ is considered in the Caputo sense [36] as:

$$\frac{d^\alpha v_Q(t)}{dt^\alpha} = \frac{1}{\Gamma(1-\alpha)}\int_0^t \frac{dv_Q(\tau)}{d\tau}\frac{d\tau}{(t-\tau)^\alpha} \tag{12}$$

which is equivalent to a convolution transform in time of $dv_Q(t)/dt$ with the power-law kernel $t^{-\alpha}/\Gamma(1-\alpha)$. In this sense, we indeed obtain $d^\alpha v_Q(t)/dt\Big|_{t\to\infty} = 0$, which leads to the same previous conclusions regarding the free term, unlike the famous Riemann-Liouville fractional-order definition [37]. Assuming the case of a constant excitation in the input (same conditions as in the case of ideal capacitor mentioned above), we can then generalize Eq. (6) [38] for the case of the CPE:

$$v_Q(t) = v_Q(\infty)\left(1 - E_\alpha\left[-\left(\frac{t}{\tau}\right)^\alpha\right]\right), \quad 0 < t < T \tag{13}$$

where the transient dynamics now is explained by the one-parameter Mittag-Leffler function defined by the following power series [39]:

$$E_\alpha\left[-\left(\frac{t}{\tau}\right)^\alpha\right] = \sum_{k=0}^{\infty}\frac{\left[-\left(\frac{t}{\tau}\right)^\alpha\right]^k}{\Gamma(\alpha k+1)}, \quad \alpha > 0 \tag{14}$$

which is a generalization of the exponential function, to which it reduces when $\alpha = 1$. We note that Eq. (12), which is a Volterra integral equation of the second kind with a singular kernel, can be solved by applying the method of successive approximation to obtain the transient response of Eq. (13) [40]. For convenience, we now separate the two components of $v_Q(t)$, the natural $v_{Q,trans}(t)$ and steady-state $v_{Q,ss}$ responses identifiable as the time-dependent and constant addends in Eq. (13), respectively. At short time scales, $v_{Q,trans}(t) \sim v_{Q,ss}$, as is the case with the ideal capacitor. Nevertheless, the problem arises for large times [41]. Mittag-Leffler function exhibits an asymptotic behavior toward zero but for an α-dependent number of time constants running to infinity [42], in stark contrast to exponential dynamics (refer to Eq. (7)), by considering the typical error bands in control engineering (from ±1% to ±5%). Conversely, if t/τ is sufficiently large, $v_Q(t)$ can be expressed in terms of the following asymptotic series expansion of the Mittag-Leffler function [43]:

$$E_\alpha\left[-\left(\frac{t}{\tau}\right)^\alpha\right] \sim \sum_{k=1}^{\infty}(-1)^{k-1}\frac{\left[-\left(\frac{t}{\tau}\right)^\alpha\right]^{-k}}{\Gamma(1-\alpha k)}, \quad \left(t/\tau\right)\to\infty \tag{15}$$

To further simplify, Eq. (15) can be rewritten by considering only the first term, yielding [44]

$$E_\alpha\left[-\left(\frac{t}{\tau}\right)^\alpha\right] \sim \frac{\left(\frac{t}{\tau}\right)^{-\alpha}}{\Gamma(1-\alpha)}, \quad \alpha \neq 1 \tag{16}$$

for which the absolute value of the second term must be much smaller that of the first, that is, $(t/\tau)^{-\alpha}/\Gamma(1-\alpha) \gg (t/\tau)^{-2\alpha}/\Gamma(1-2\alpha)$ or

$$\left(\frac{t}{\tau}\right) \gg \left[\frac{\Gamma(1-\alpha)}{\Gamma(1-2\alpha)}\right]^{1/\alpha} \tag{17}$$

which holds true in the vast majority of experimental cases.

At sufficiently long times satisfying the constraint imposed by Eq. (17), we can therefore consider the approximation involved in Eq. (16) and rewrite the voltage across the fractional-order capacitor given by Eq. (13) as follows:

$$v_Q(t) = v_Q(\infty)\left[1 - \frac{(t/\tau)^{-\alpha}}{\Gamma(1-\alpha)}\right], \quad 0 < t < T, \quad \left(t/\tau\right)\to\infty \tag{18}$$

The dynamics associated with the term $(t/\tau)^{-\alpha}$ can conceptually arise from the summation of many different exponential decays $e^{-t/\tau}$, each making a different contribution inversely proportional to the time constant raised to the power $1-\alpha$ [45]; that is, $\tau^{1-\alpha}$. In effect, it is well-known that the inverse power-law behavior plays a universal role of relaxation dielectric processes in nature [46].

Same as for the case of the capacitor, $v_{Q,trans}(t)$ also decays to zero as time progresses. However, the Mittag-Leffler pattern requires a high number of time constants to consider this function equals to zero [24,47], as commented on previously. In any case, by steady-state response, we mean the response that exits after the transient terms are negligible; i.e., $v_{Q,trans}(t) \ll v_{Q,ss}$ [42]. This condition can be arranged from Eq. (18), yielding

$$t_{ss,Q} = \tau\left[e^{-4}\Gamma(1-\alpha)\right]^{-1/\alpha} \tag{19}$$

obtaining thus the steady-state time, beyond which the step response $v_Q(t)$ does not differ from the final value $v_Q(\infty)$ by more than ±2%, as depicted in Fig. 1(a). At this point, it should be clear that Eqs. (7) and (19) establish steady-state times on the internal capacitive variables. However, it is possible that external variables may require slower time intervals to reach the equilibrium regime due to the resistive configuration of the circuit [41,48]. In Appendix A, a generalization of our

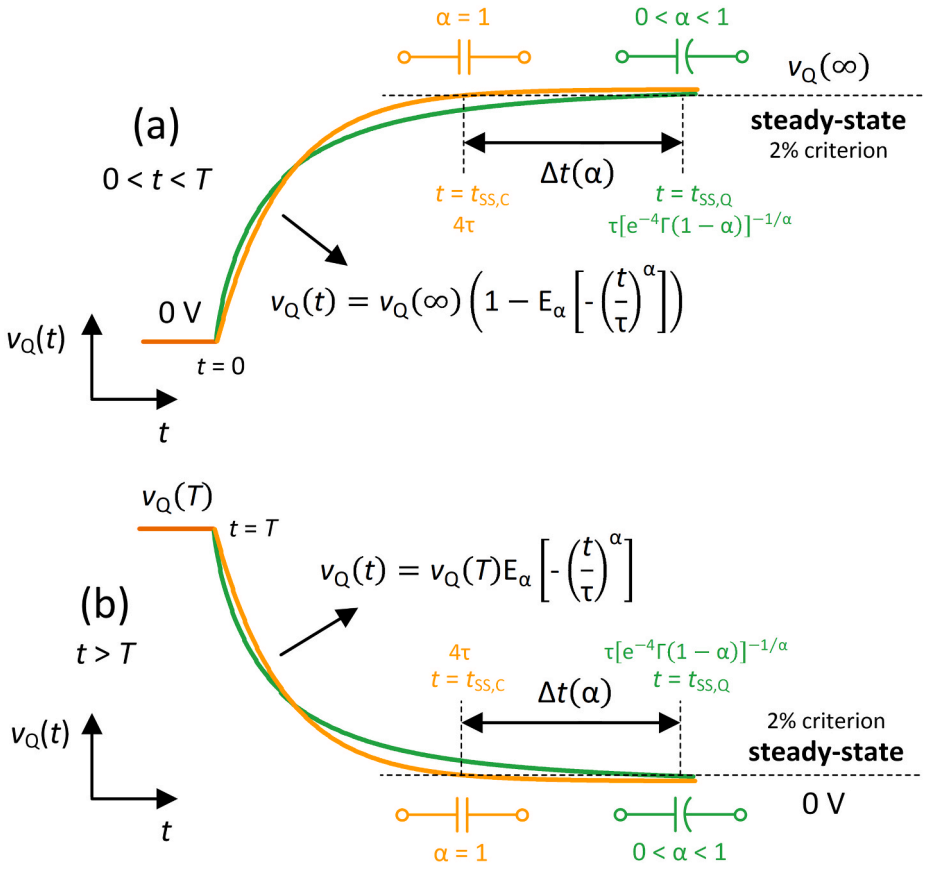

Fig. 1. Illustration of time-voltage profiles of (a) charging and (b) discharging classical ($\alpha = 1$) or anomalous ($0 < \alpha < 1$) capacitive energy storage materials.

theory is formulated for the case of a step-response of voltage-excited Randles circuits.

From a mathematical perspective, it is evident that an exponential relaxation exhibits a faster decay than the fractional one given by the Mittag-Leffler function for large times,

$$e^{-t/\tau} < E_\alpha\left[-\left(\frac{t}{\tau}\right)^\alpha\right], \quad \left(t/\tau\right)\to\infty \tag{20}$$

which suggests that the fractional-order capacitor represents a delayed version of the ideal one because the time needed to reach a fully charged state, $t_{ss,Q} > t_{ss,C}$. Note that $e^{-t/\tau} > E_\alpha\left[-\left(t/\tau\right)^\alpha\right]$ at short time scales, in contrast to Eq. (20). Thus, if one replaces the time difference $t_{ss,Q} - t_{ss,C}$ by a new α-dependent variable $\Delta t(\alpha)$ obtained from Eqs. (7) and (19), according to

$$\Delta t(\alpha) = t_{ss,Q} - t_{ss,C} = 4R_{Th}\Delta C(\alpha) \tag{21}$$

emerges therefore a term based on the concept of "differential capacitance" that quantifies the deviation from ideality ($\alpha = 1$, $Q = C$) to the real capacitance of the CPE. Hence, we obtain

$$\Delta C(\alpha) = C_{limit}(\alpha) - C \tag{22}$$

where

$$C_{limit}(\alpha) = \frac{C_{eff}}{4[e^{-4}\Gamma(1-\alpha)]^{1/\alpha}} \tag{23}$$

$$C_{eff} = Q^{1/\alpha}R_{Th}^{(1-\alpha)/\alpha} \tag{24}$$

Eq. (23) is found by equating Eqs. (7) and (19) as $4R_{Th}C_{limit}(\alpha) = \tau[e^{-4}\Gamma(1-\alpha)]^{-1/\alpha}$ and substituting for τ from Eq. (11) and the ratio $Q^{1/\alpha}R_{Th}^{(1-\alpha)/\alpha}$ from the famous formula of the effective capacitance of the CPE (refer to Eq. (24)) [49]. Here, the concept of "limit capacitance of a CPE" is a general denomination for a class of dynamical models, present in many processes and materials, caused by a delay effect on the physical phenomena and visible in impedance and transient responses at long time scales [50]. Both C_{eff} and $C_{limit}(\alpha)$ are, in any case, virtual capacitances that provide a helpful description of real-world processes under ideal comprehensive conditions.

It is noteworthy to mention that the analysis presented above remains the same for the case of discharge:

$$v_Q(t) = \begin{cases} v_Q(T)E_\alpha\left[-\left(\frac{t}{\tau}\right)^\alpha\right], & t > T \\ v_Q(T)\frac{(t/\tau)^{-\alpha}}{\Gamma(1-\alpha)}, & t > T, \quad \left(t/\tau\right)\to\infty \\ 0, & t > T, \quad t \geq t_{ss,Q} \end{cases} \tag{25}$$

with the unique difference that, in the charge phase, a non-zero residual capacitive-nature current results in $v_Q(t)$ [51,52] being lower than the steady-state value ($v_Q(t) < v_Q(\infty)$ for $0 < t < T$) if $T < t_{ss,Q}$. In contrast, the voltage across the dissipative capacitor in the discharging is higher than the equilibrium level (always $v_Q(t) > 0$ for $t > T$) due to negative remanent currents, as demonstrated in Fig. 1(b). Note that, in effect, the CPE exhibits, in an approximate way, some basic properties shown by classic capacitor theory (memory or continuity) in the transient behavior, which are essential for the analysis of distributed-parameter electrical circuits by inspection.

Regarding the nature of physical events in real energy storage devices, even more complex situations can be expected experimentally

leading to overlapping processes with slow fractional-order traces that rule the long timescale phenomena under certain circumstances [29]. These additional characteristics need to be described more accurately by a more general model, but, in any case, the time delay for the charge/discharge processes can be derived in the same spirit by focusing on the slowest mechanism governing the response (RC *vs* R-CPE subcircuit) if the respective characteristic time scales are well separated. Otherwise, the fractional dynamics should be modeled by using the Prabhakar function $\mathrm{E}^{\gamma}_{\alpha,\beta}[-(t/\tau)^{\alpha}] = (1/\Gamma(\gamma))\sum_{k=0}^{\infty}\frac{\Gamma(\gamma+k)[-(t/\tau)^{\alpha}]^{k}}{k!\Gamma(\alpha k+\beta)}$, $\alpha,\beta,\gamma>0$ [53], complicating the analysis developed here and which is beyond the scope of this work. If one, on the other hand, considers a dynamic equivalent circuit constituted by an unlimited number of RC branches to model the distribution of capacitance, each subcircuit is associated with a relation time τ_i which leads to an infinite summation of exponential transient terms $\sum_i e^{-t/\tau_i}$. Therefore, this discrete model suggests a prolonged decay over an unrestricted time scale, which is not physically reasonable [23,50,54]. Although many references assume the CPE-type of response to be over an infinite frequency range in the electrical modeling of electrochemical power sources, they must actually deviate from such behavior at extremely low frequencies. Thus, we here obtain a unified steady-state time for the CPE that limits the charge of the energy storage devices in order to yield realistic realizable responses from the concept of "incremental capacitance" by comparing the classical and fractional-order capacitor at long time scales.

Fig. 2 gives an overview of how the time delay $\Delta t(\alpha)$ depends on α. As the dispersion coefficient decreases, the time delay for reaching an equilibrium state increases, which is consistent with the deceleration level of the transient responses shown in Fig. 1. The transition from the ideal capacitor to the Warburg behavior is completed in almost three decades of time, requiring thus several tens of additional seconds to charge/discharge a real-world energy storage material (CPE behavior with α commonly varying around 0.65 and 0.95 shown in the inset of Fig. 2) in comparison to the conventional capacitor. However, we should point out that if the accuracy at steady-state operation is not of prime importance in a device under study, then we should not require unnecessarily large time delays to consider the transient response as negligible, since such stringent specifications could be alleviated with lower tolerance values (e.g., ±5% of typical use in control engineering [12]). To derive our mathematical theory, we therefore established as a premise the compromise between the simplicity of the model and the accuracy of the results, leading, in practice, to a good agreement between simulated and experimental studies. Note that, importantly, the

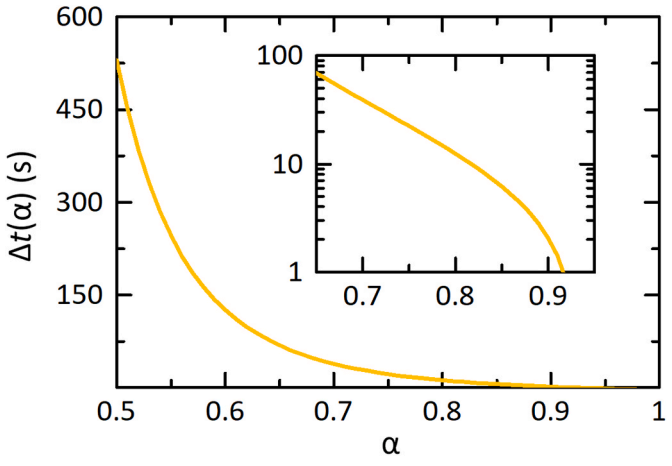

Fig. 2. Time delay $\Delta t(\alpha)$ required for the charging/discharging of a real-world device in relation to the ideal non-dispersive view by considering a Thévenin resistance of 0.5 Ω and a CPE parameter with a value of 1.5 $F/s^{1-\alpha}$.

analysis developed here is equally valid for anomalous inductive phenomena [55], also visible in complex energy-related materials [56,57].

From the previous theoretical analysis, explicit solutions to the charge, power and energy behavior at long time scales for real-world capacitive devices can be derived by taking into account their fractional-order dynamics. Classical equations of an ideal capacitor ($\alpha = 1$), such as $q = Cv$, $p = Cv\,\mathrm{d}v/\mathrm{d}t$, and $W = \frac{1}{2}Cv^2$ cannot be true for the CPE ($0<\alpha<1$), thus making it necessary to return to the basic mathematical relationships of circuit theory and reformulate the problem for the new steady-state time given by Eq. (19). Charge for the generalized capacitance modeled by Eq. (9) following a step-input excitation can be obtained by integrating the current as $q = \int_0^{t_{ss,Q}} i_Q \mathrm{d}t$. The respective electrical power and energy analyses in pseudo-equilibrium conditions now follow the expressions $p = v\left(Q\,\mathrm{d}^{\alpha}v_Q/\mathrm{d}t^{\alpha}\right)$ and $W = Q\int_0^{t_{ss,Q}} v_Q \mathrm{d}^{\alpha}v_Q/d\tau^{\alpha}\,d\tau$. Indeed, closed-form analytical solutions for charge, power and energy have already been reported in literature from the theory of fractional calculus [25,56]. Unlike the ideal capacitor where all the circuit variables are governed by the exponential function $e^{-t/\tau}$ in first-order circuits, here the situation becomes more complex due to the recurrence properties of the Mittag-Leffler function [39]; that is, the *m*-th derivative/anti-derivative of the classical Mittag-Leffler function, $\left(\mathrm{d}/\mathrm{d}t\right)^{m}\mathrm{E}_{\alpha}[-(t/\tau)^{\alpha}] = t^{\beta-m-1}\mathrm{E}_{\alpha,\beta-m}[-(t/\tau)^{\alpha}]$, is expressed in terms of the two-parametric Mittag-Leffler function $\mathrm{E}_{\alpha,\beta}[-(t/\tau)^{\alpha}] = \sum_{k=0}^{\infty}\frac{[-(t/\tau)^{\alpha}]^{k}}{\Gamma(\alpha k+\beta)}$, $\alpha,\beta>0$. Such transient dynamics in charge, power and energy do not however converge to a final value ($q, p, W \to \infty$) because $\mathrm{E}_{\alpha,\beta}[-(t/\tau)^{\alpha}]$ is multiplied by the time, leading to the need to "stop" the response at a certain time instant (here determined as $t = t_{ss,Q}$). Thus, our work provides a reformulation of transient-based characterization tests used for energy storage devices, eliminating inconsistencies in industrial/academic standards on the proper way to charge/discharge such materials.

3. Experimental procedure

We select one representative energy storage device with evident dispersive behavior for an experimental study, such as the supercapacitor, as reflected by literature results [26]. Indeed, the use of supercapacitors in electrical circuits requires accurate protocols for their proper characterization from charging and discharging sequences, as the one developed here. The electrical measurements were performed on a 3 F, 2.7 V Cooper Bussmann PowerStor supercapacitor and a 3 F, 2.7 V GHC Nanoforce device using an Autolab PGSTAT204 Potentiostat/Galvanostat (Metrohm). Characteristics of the electric double-layer capacitors (EDLCs), specified by the manufacturer, are listed in Table 1. In each case, the current in the device was recorded beginning at the instant a rectangular voltage pulse of a height of 1 V is applied until the time at which the subsequent relaxation process approaches to zero. A sampling rate of 0.2 MHz was used, and all the experiments were

Table 1
Characteristics of the supercapacitors supplied by the manufacturer.

Fabricant	Capacitance (F)	Maximum initial ESR (mΩ)	Maximum working voltage (V)
Cooper Bussmann PowerStor	3	80	2.7
GHC Nanoforce	3	100	2.7

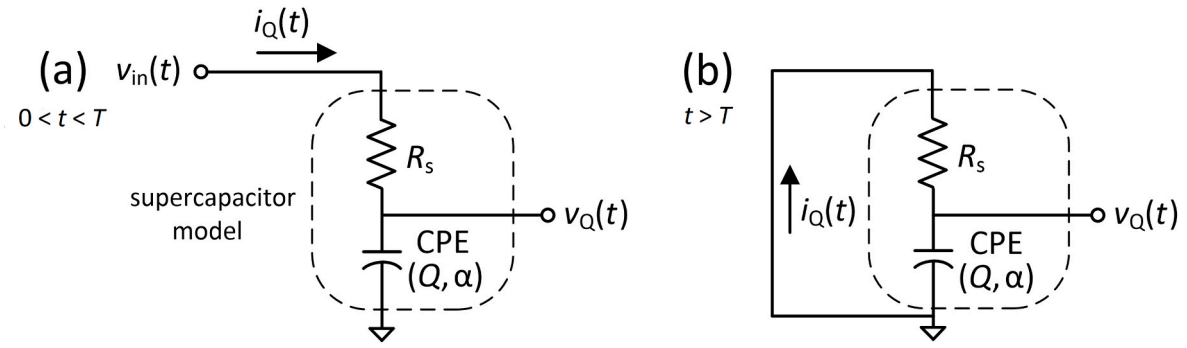

Fig. 3. Electrical circuits for (a) charging and (b) discharging the fractional model of an electric double layer capacitor (EDLC).

repeated five consecutive times on each supercapacitor.

4. Results and discussion

A simple circuit that can be used to obtain the step-excited voltage response of a fractional-order capacitor is shown in Fig. 3(a), where the EDLC, modeled by an internal ohmic resistance R_s in series with a physics-based CPE, is charged at the electric potential $v_{in}(t) = V$. For this case, $R_{Th} = R_s$ and $\tau = (R_s Q)^{1/\alpha}$. On the other hand, Fig. 3(b) shows the self-discharge of the device into the series resistance. The selection of supercapacitors here is justified because, in most real-world materials tested in science, the capacitive element is an internal part of a general equivalent circuit [51,58–60], being thus experimentally inaccessible for the study of its anomalous dynamics.

Before proceeding to experiments, we will derive the mathematical expressions for the transient-current response under stepped operation. Once the transient voltages have been determined corresponding to the charge and discharge phases, we can easily derive the expressions of the current $i_Q(t)$, for $0 < t < T$ and $t > T$, from Eqs. (9), (13) and (25) as:

$$i_Q(t) = \begin{cases} \frac{v_Q(\infty)}{R_{Th}} \mathrm{E}_\alpha\left[-\left(\frac{t}{\tau}\right)^\alpha\right], & 0 < t < T \quad (26a) \\ -\frac{v_Q(T)}{R_{Th}} \mathrm{E}_\alpha\left[-\left(\frac{t}{\tau}\right)^\alpha\right], & t > T \quad (26b) \end{cases} \tag{26}$$

Here, $i_Q(t)$ exhibits an undershoot of value

$$i_Q(T^+) - i_Q(T^-) = -\left(\frac{v_Q(T)}{R_{Th}} + \frac{v_Q(\infty)}{R_{Th}} \mathrm{E}_\alpha\left[-\left(\frac{T}{\tau}\right)^\alpha\right]\right) \tag{27}$$

at the instant $t = T$ and then it starts a Mittag-Leffler rise toward zero (see below). Indeed, $i_Q(t)$ exhibits the same relaxation pattern, in terms of the Mittag-Leffler function, validating the use of Eqs. (19)–(24) for the evaluation of the steady-state regime. Note that, theoretically speaking, the area of current waveform above the zero axis should be equal to that below for a total average value of zero if $T \geq t_{ss,Q}$ ($i_Q(T^+) - i_Q(T^-) = -v_Q(T)/R_{Th}$ in Eq. (27)) under LTI conditions. Nevertheless, the transient responses in supercapacitors have been commonly found asymmetric looking at the charge and discharge sequences under pulsed operation in the literature, attributed to irreversible processes such as different regimes at the anodic and cathodic sides of the devices [28].

Firstly, we study the Powerstor supercapacitor in response to the step voltage $V = 1$ V. The waveform of the resulting current $i_Q(t)$ flowing through the non-ideal capacitive energy storage device for $t > 0$ is sketched in Fig. 4(a), where the blue line indicates $i_Q(t)$ for $\alpha = 1$ (exponential behavior). In fact, the distributed relaxation dynamics exhibits a faster decay than the ideal one, for short times. However, the inherent fractional-order nature of supercapacitors introduces a significant deceleration in the transient response, being thus slower than the

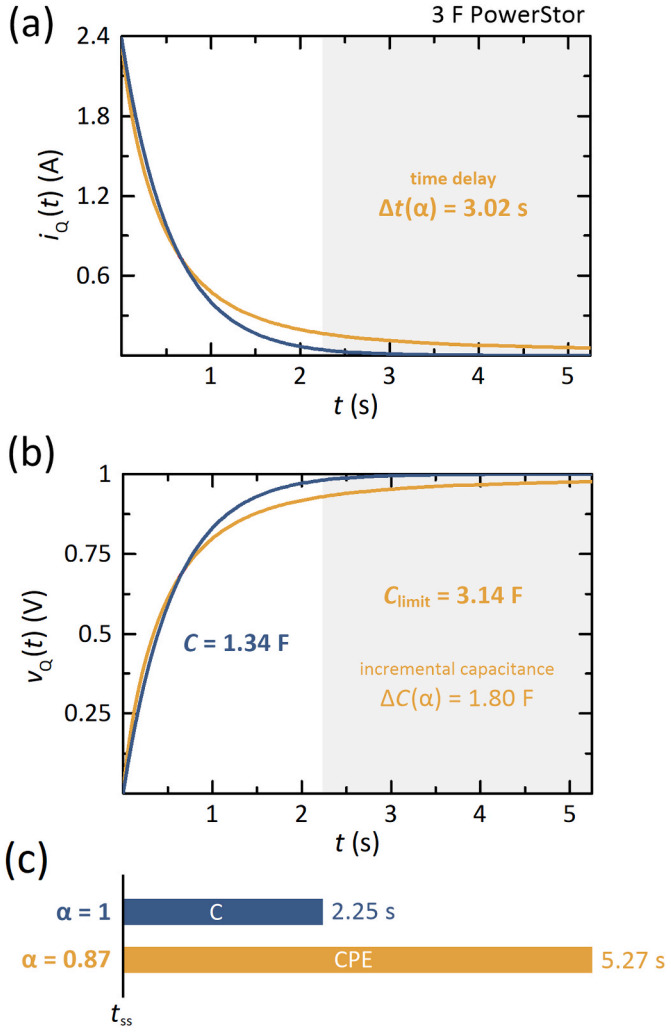

Fig. 4. (a) Current and (b) voltage waveforms in response to a step voltage with height $V = 1$ V and duration T applied to a Powerstor supercapacitor under real conditions ($0 < \alpha < 1$) and considering $\alpha = 1$ (exponential behavior). Parameters obtained via fitting procedure to the equivalent circuits shown in Fig. 3 are also shown, including the steady-state times for both cases in (c).

exponential dynamics at long time scales. The internal voltage across the capacitor of fractional nature, plotted in Fig. 4(b) and calculated as $v_Q(t) = V - i_Q(t)R_s$, exhibits the same transient dynamics as the current (also in comparison to ideal behavior, indicated again in blue line) being now a non-exponential rise rather instead of a decay. Although apparently the experimental-voltage waveform could be more or less

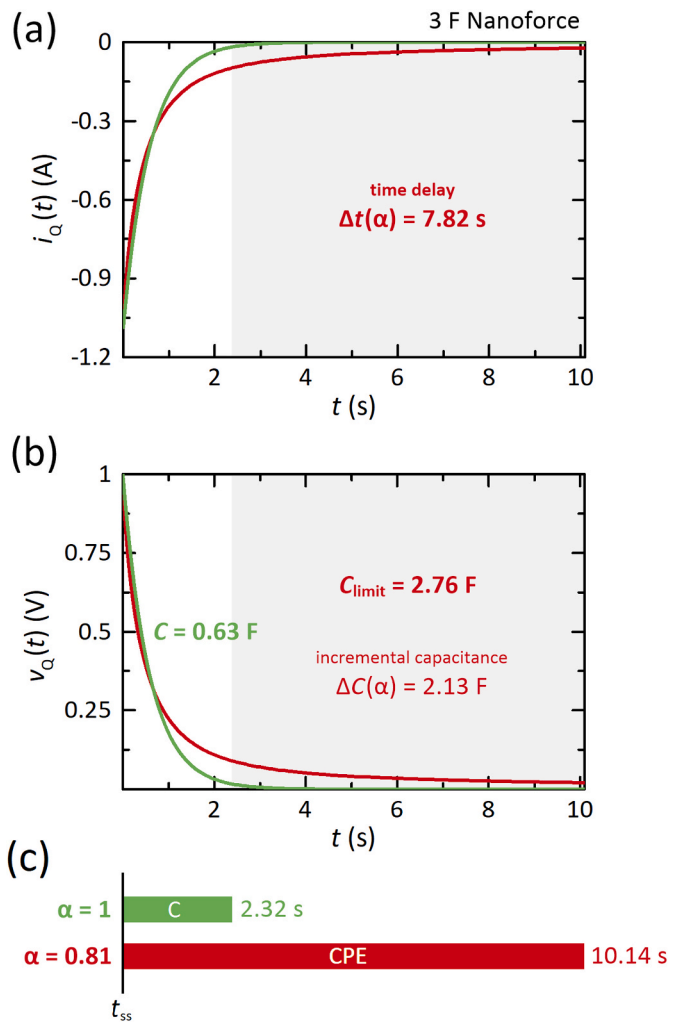

Fig. 5. (a) Waveforms of the ulterior (a) transient current $i_Q(t)$ and (b) voltage $v_Q(t)$, together with the obtained parameter values, in response to a voltage of a 1 V applied into the Nanoforce EDLC. Plots considering the R_s-C model are also shown using green lines in (a) and (b). (c) Comparison of the steady-state times $t_{ss,C}$ and $t_{ss,Q}$ by using $\alpha = 1$ and $\alpha = 0.81$, respectively. (For interpretation of the references to colour in this figure legend, the reader is referred to the Web version of this article.)

inherited from traditional capacitors theory, the reality is that the use of the classical formulation (Eqs. (1)–(8)) inevitably leads to tremendous errors in the characterization. The R_s-CPE fitting parameters are found to be $R_s = 0.42\ \Omega$, $Q = 1.34\ \mathrm{F/s^{1-\alpha}}$, and $\alpha = 0.87$, similarly to Refs. [26,27,61]. The effective and limit capacitances calculated using Eqs. (23) and (24), respectively, result in $C_{eff} = 1.23$ F and $C_{limit}(\alpha) = 3.14$ F. Even though the time constant exhibits a low value ($\tau = 0.52$ s), an elapsed time of more than ten time constants ($t_{ss,Q} = 5.28$ s) is required for the electrical responses to reach the equilibrium for the 2% criterion. Due to the effect of α on the transient dynamics of real-world supercapacitive energy storage materials, conveniently represented in the representative examples of Fig. 4(a) and (b), the charge time increases, in comparison to the ideal behavior, according to Eq. (21), $\Delta t(\alpha) = 3.02$ s, which represents a 134% increase over the value of $t_{ss,C}$, as illustrated in Fig. 4(c). In other words, CPE effects provide an *incremental capacitance* with respect to the ideal behavior ($\alpha = 1$, $Q = C$) of $\Delta C(\alpha) = 1.80$ F, which logically slows down the transient dynamics.

Fig. 5(a) shows the experimental current transient just after turning off an input voltage of $V = 1$ V for the Nanoforce EDLC. After the negative initial peak due to the device's capacitive effects, $i_Q(T^+) = -{}^1/_{R_s}$, the current increases because the CPE discharges through the series resistance. Note that, at instant $t = T^-$ (just before the voltage is switched off), $i_Q(T^-) = 0$ A which is the steady-state value ($T \geq t_{ss,Q}$). In this representative example, it can be easily appreciated a fractional dynamics, which is slower the smaller the dispersive coefficient, as for the case of the internal voltage $v_Q(t)$ (see Fig. 5(b)). The specific cases in which $\alpha = 1$ (ideal capacitor) have also been also plotted. Experimental values obtained from the fitting analysis were $R_s = 0.92\ \Omega$, $Q = 0.63\ \mathrm{F/s^{1-\alpha}}$, $\alpha = 0.81$, $\tau = 0.51$ s, $C_{eff} = 0.55$ F, and $C_{limit}(\alpha) = 2.76$ F. A close inspection of the calculated electrical quantities reveals a high degree of deceleration of $i_Q(t)$ and $v_Q(t)$ because a 2% steady-state time of $t_{ss,Q} = 10.14$ s, due to an increment of capacitance of $\Delta C(\alpha) = 2.13$ F, is indeed necessary to the current response enters and remains within our specified tolerance band. By comparing the two transient curves (ideal and anomalous behavior) for $i_Q(t)$ and $v_Q(t)$, the effect of the time delay observed for sufficiently long times, $\Delta t(\alpha) = 7.82$ s, is noticeable as can be seen in Fig. 5(c), since one would obtain a large relative error of 77% for the charging time calculated from the conventional R_s-C-based formulae (refer to Eq. (7)).

5. Conclusions

In this paper, a realistic dynamical model for the charging/discharging time of capacitive energy storage devices have been derived and experimentally verified on two commercial supercapacitors with a clear dispersive nature. Our theory describes the steady-state operation in voltage and current of this type of devices that commonly show a transformation from the integer- (ideality described in practical documentation) to fractional-order (reality found in experimental measurements) capacitive behavior, thus introducing an increment in the duration of transient effects. Indeed, fractional dynamics modifies standard exponential processes and gives rise to the Mittag-Leffler relaxation with an intrinsic decelerated behavior at long time scales due to its asymptotic properties. Therefore, we presented here the recommended procedure to be applied for complete charging/discharging the internal capacitance of energy storage materials in the time domain, which is consistent with the frequency-domain impedance reports found in literature.

CRediT authorship contribution statement

Enrique H. Balaguera: Writing – review & editing, Writing – original draft, Visualization, Validation, Supervision, Software, Project administration, Methodology, Investigation, Funding acquisition, Formal analysis. **Anis Allagui:** Writing – review & editing, Validation, Resources, Formal analysis, Conceptualization.

Declaration of competing interest

The authors declare that they have no known competing financial interests or personal relationships that could have appeared to influence the work reported in this paper.

Data availability

Data will be made available on request.

Acknowledgements

This work has received funding from the Universidad Rey Juan Carlos, project number M2993.

Appendix A. General theory for the Randles circuit under potentiostatic control

Here, we want to discuss our theory in the context of the Randles circuit [62]. In this famous model, an additional resistance R_p emerges connected in parallel to the capacitive element. However, when analyzing the steady-state transient current response under a potentiostatic control, this apparently simple procedure becomes, in practice, a difficult task, involving extensive reformulation in the estimation of $\Delta t(\alpha)$, especially if $R_p \gg R_s$ [41]. Considering the ideal Randles circuit ($\alpha = 1$), the steady-state time [63] is now

$$t_{ss,C} = \tau\left[4 - \ln\left(\frac{R_s}{R_p}\right)\right] \tag{A.1}$$

which broads the classical expression given by Eq. (7), where it is considered $R_p \to \infty$. On the other hand, a settling reference value of $t_{ss,Q}$, for the case of the modified Randles circuit ($0 < \alpha < 1$) [48,64], is obtained as

$$t_{ss,Q} = \tau\left[\frac{e^{-4}\Gamma(1-\alpha)}{R_p/R_s}\right]^{-1/\alpha} \tag{A.2}$$

Thus, the ratio R_s/R_p will introduce slight changes in the formulation of the problem. The additional potential-step hold time, $\Delta t(\alpha) = t_{ss,Q} - t_{ss,C}$, is given, in this scenario, by

$$\Delta t(\alpha) = 4R_{TH} f\left(\alpha, Q, R_s/R_p\right) \tag{A.3}$$

where $f\left(\alpha, Q, R_s/R_p\right)$ represents a general resistive-capacitive function of the Randles circuits that generalize Eq. (22) as

$$f\left(\alpha, Q, R_s/R_p\right) = \frac{C_{limit}(\alpha)}{\left(R_s/R_p\right)^{1/\alpha}} - C\left[1 - \frac{1}{4}\ln\left(\frac{R_s}{R_p}\right)\right] \tag{A.4}$$

Interestingly, if the resistive configuration of the circuit under study involves that $R_p \gg R_s$, hold times substantially increase due to the fact that the initial current flowing through the CPE is extremely higher than the steady-state current, $V/R_s \gg V/R_s + R_p$ [41], requiring thus a superior number of time constants to reach the equilibrium in the external current. In effect, this advanced analysis does not have implications in the calculation of the time delay in the steady-state dynamics of the fractional-order capacitor but rather for the variable measured in the specific case of voltage-excited parallel RC (or R-CPE) circuits.

References

[1] J. Liu, J. Wang, C. Xu, H. Jiang, C. Li, L. Zhang, J. Lin, Z.X. Shen, Advanced energy storage devices: basic principles, analytical methods, and rational materials design, Adv. Sci. 5 (2018) 1700322.
[2] J. Zhao, A.F. Burke, Electrochemical capacitors: materials, technologies and performance, Energy Storage Mater. 36 (2021) 31–55.
[3] J.W. Nilsson, S.A. Riedel, Electric Circuits, Pearson, 2019.
[4] L. Chua, O.A. Desoear, Linear and Non Linear Circuits, McGraw-Hill Education, 2000.
[5] E. Barsoukov, J.R. Macdonald, Impedance Spectroscopy: Theory, Experiment, and Applications, John Wiley & Sons, 2005.
[6] J.R. Macdonald, Impedance spectroscopy, Ann. Biomed. Eng. 20 (1992) 289–305.
[7] V. Vivier, M.E. Orazem, Impedance analysis of electrochemical systems, Chem. Rev. 122 (2022) 11131–11168.
[8] F.F. Kuo, Network Analysis and Synthesis, John Wiley & Sons, 1966.
[9] A.A. Moya, Identification of characteristic time constants in the initial dynamic response of electric double layer capacitors from high-frequency electrochemical impedance, J. Power Sources 397 (2018) 124–133.
[10] E. Hernández-Balaguera, J. Bisquert, Time transients with inductive loop traces in metal halide perovskites, Adv. Funct. Mater. 34 (6) (2024) 2308678.
[11] A.S. Sedra, K.C. Smith, Microelectronic Circuits, Oxford University Press, 2004.
[12] K. Ogata, Modern Control Engineering, Prentice Hall, 2010.
[13] C. Zou, L. Zhang, X. Hu, Z. Wang, T. Wik, M. Pecht, A review of fractional-order techniques applied to lithium-ion batteries, lead-acid batteries, and supercapacitors, J. Power Sources 390 (2018) 286–296.
[14] J.I. Hidalgo-Reyes, J.F. Gómez-Aguilar, R.F. Escobar-Jiménez, V.M. Alvarado-Martínez, M.G. López-López, Classical and fractional-order modeling of equivalent electrical circuits for supercapacitors and batteries, energy management strategies for hybrid systems and methods for the state of charge estimation: a state of the art review, Microelectron. J. 85 (2019) 109–128.
[15] Y. Wang, M. Li, Z. Chen, Experimental study of fractional-order models for lithium-ion battery and ultra-capacitor: modeling, system identification, and validation, Appl. Energy 278 (2020) 115736.
[16] A.K. Jonscher, The interpretation of non-ideal dielectric admittance and impedance diagrams, Phys. Status Solidi 32 (1975) 665–676.
[17] D.D. Macdonald, Reflections on the history of electrochemical impedance spectroscopy, Electrochim. Acta 51 (2006) 1376–1388.
[18] K.S. Cole, Permeability and impermeability of cell membranes for ions, cold spring harb symp quant, Biol. 8 (1940) 110–122.
[19] S. Westerlund, L. Ekstam, Capacitor theory, IEEE Trans. Dielectr. Electr. Insul. 1 (1994) 826–839.
[20] G.J. Brug, A.L.G. van den Eeden, M. Sluyters-Rehbach, J.H. Sluyters, The analysis of electrode impedances complicated by the presence of a constant phase element, J. Electroanal. Chem. Interfacial Electrochem. 176 (1984) 275–295.
[21] C.H. Hsu, F. Mansfeld, Technical note: concerning the conversion of the constant phase element parameter Y0 into a capacitance, Corrosion 57 (2001) 747–748.
[22] A. Lasia, The origin of the constant phase element, J. Phys. Chem. Lett. 13 (2022) 580–589.
[23] A. Sadkowski, Time domain responses of constant phase electrodes, Electrochim. Acta 38 (1993) 2051–2054.
[24] R. Metzler, J. Klafter, From stretched exponential to inverse power-law: fractional dynamics, Cole–Cole relaxation processes, and beyond, J. Non-Cryst. Solids 305 (2002) 81–87.
[25] A. Allagui, T.J. Freeborn, A.S. Elwakil, B.J. Maundy, Reevaluation of performance of electric double-layer capacitors from constant-current charge/discharge and cyclic voltammetry, Sci. Rep. 6 (2016) 38568.
[26] A. Allagui, T.J. Freeborn, A.S. Elwakil, M.E. Fouda, B.J. Maundy, A.G. Radwan, Z. Said, M.A. Abdelkareem, Review of fractional-order electrical characterization of supercapacitors, J. Power Sources 400 (2018) 457–467.
[27] M.E. Fouda, A. Allagui, A.S. Elwakil, A. Eltawil, F. Kurdahi, Supercapacitor discharge under constant resistance, constant current and constant power loads, J. Power Sources 435 (2019) 226829.
[28] T.J. Freeborn, B. Maundy, A.S. Elwakil, Measurement of supercapacitor fractional-order model parameters from voltage-excited step response, IEEE J. Emerg. Sel. Top. Circuits Syst. 3 (3) (2013) 367–376.
[29] T.J. Freeborn, B. Maundy, A.S. Elwakil, Fractional-order models of supercapacitors, batteries and fuel cells: a survey, Mater, Renew. Sustain. Energy 4 (2015) 9.
[30] K. Abro, P. Shaikh, J.F. Gómez-Aguilar, I. Khan, Analysis of De-Levie's model via modern fractional differentiations: an application to supercapacitor, Alex. Eng. Journal 58 (2019) 1375–1384.
[31] J.A. López Villanueva, P. Rodríguez Iturriaga, L. Parrilla Roure, S. Rodríguez Bolívar, A compact model of the ZARC for circuit simulators in the frequency and time domains, AEU Int. J. Electron. Commun. 153 (2022) 154293.
[32] L.E. Helseth, Modelling supercapacitors using a dynamic equivalent circuit with a distribution of relaxation times, J. Energy Storage 25 (2019) 100912.

[33] M.A. Danzer, Generalized distribution of relaxation times analysis for the characterization of impedance spectra, Batteries 5 (3) (2019) 53.
[34] F. Ciucci, Modeling electrochemical impedance spectroscopy, Curr. Opin. Electrochem. 13 (2019) 132–139.
[35] B.A. Boukamp, Distribution (function) of relaxation times, successor to complex nonlinear least squares analysis of electrochemical impedance spectroscopy? JPhys Energy 2 (2020) 042001.
[36] I. Podlubny, Fractional Differential Equations: an Introduction to Fractional Derivatives, Fractional Differential Equations, to Methods of Their Solution and Some of Their Applications, Academic Press, 1998.
[37] H. Rudolf, Applications of Fractional Calculus in Physics, World Scientific, 2000.
[38] M.D. Ortigueria, V. Martynyuk, V. Kosenkov, A.G. Batista, A new look at the capacitor theory, Fractal Fract 7 (2023) 86.
[39] R. Gorenflo, A.A. Kilbas, F. Mainardi, S.V. Rogosin, Mittag-Leffler Functions, Related Topics and Applications, Springer-Verlag, 2014.
[40] F.H. van Heuveln, Analysis of nonexponential transient response due to a constant-phase element, J. Electrochem. Soc. 141 (1994) 3423.
[41] E. Hernández-Balaguera, J.L. Polo, On the potential-step hold time when the transient-current response exhibits a Mittag-Leffler decay, J. Electroanal. Chem. 856 (2020) 113631.
[42] E. Hernández-Balaguera, Numerical approximations on the transient analysis of bioelectric phenomena at long time scales via the Mittag-Leffler function, Chaos, Solit. Fractals 145 (2021) 110768.
[43] A. Erdélyi, Higher Transcendental Functions, McGraw-Hill, 1955.
[44] F. Mainardi, On some properties of the Mittag-Leffler function $E\alpha(-t^{\alpha})$ completely monotone for $t>0$ with $0<\alpha<1$, Discrete Contin, Dyn. Syst. Int. J. B 19 (2014) 2267.
[45] J. Thorson, M. Biederman-Thorson, Distributed relaxation processes in sensory adaptation, Science 183 (1974) 161–172.
[46] A.K. Jonscher, The 'universal' dielectric response, Nature 267 (1977) 673–679.
[47] R. Garrappa, F. Mainardi, M. Guido, Models of dielectric relaxation based on completely monotone functions, Fract. Calc. Appl. Anal. 19 (2016) 1105–1160.
[48] E. Hernández-Balaguera, L. Muñoz-Díaz, C. Pereyra, M. Lira-Cantú, M. Najafi, Y. Galagan, Universal control strategy for anomalous ionic-electronic phenomenology in perovskite solar cells efficiency measurements, Mater. Today Energy 27 (2022) 101031.
[49] B. Hirschorn, M.E. Orazem, B. Tribollet, V. Vivier, I. Frateur, M. Musiani, Determination of effective capacitance and film thickness from constant-phase-element parameters, Electrochim. Acta 55 (2010) 6218–6227.
[50] E.H. Balaguera, A. Allagui, Limit capacitance of the constant phase element, J. Energy Storage 90 (2024) 111801.
[51] E. Hernández-Balaguera, J.L. Polo, A generalized procedure for the coulostatic method using a constant phase element, Electrochim. Acta 233 (2017) 167–172.
[52] E. Hernández-Balaguera, Coulostatics in bioelectrochemistry: a physical interpretation of the electrode-tissue processes from the theory of fractional calculus, Chaos, Solit. Fractals 145 (2021) 110787.
[53] R. Garra, R. Garrappa, The prabhakar or three parameter mittag–leffler function: theory and application, Commun. Nonlinear Sci. Numer. Simulat. 56 (2018) 314–329.
[54] J. Ross Macdonald, Note on the parameterization of the constant-phase admittance element, Solid State Ionics 13 (1984) 147–149.
[55] E. Hernández-Balaguera, Fractional model of the chemical inductor, Chaos, Solit. Fractals 172 (2023) 113470.
[56] M.E. Fouda, A.S. Elwakil, A.G. Radwan, A. Allagui, Power and energy analysis of fractional-order electrical energy storage devices, Energy 111 (2016) 785–792.
[57] E. Hernández-Balaguera, B. Arredondo, C. Pereyra, M. Lira-Cantú, Parameterization of the apparent chemical inductance of metal halide perovskite solar cells exhibiting constant-phase-element behavior, J. Power Sources 560 (2023) 232614.
[58] E. Hernández-Balaguera, E. López-Dolado, J.L. Polo, Obtaining electrical equivalent circuits of biological tissues using the current interruption method, circuit theory and fractional calculus, RSC Adv. 6 (2016) 22312–22319.
[59] E. Hernández-Balaguera, H. Vara, J.L. Polo, Identification of capacitance distribution in neuronal membranes from a fractional-order electrical circuit and whole-cell patch-clamped cells, J. Electrochem. Soc. 165 (12) (2018) G3104–G3111.
[60] E. Hernández-Balaguera, B. Romero, M. Najafi, Y. Galagan, Analysis of light-enhanced capacitance dispersion in perovskite solar cells, Adv. Mater. Interfaces 9 (9) (2022) 2102275.
[61] M.E. Fouda, A.S. Elwakil, A. Allagui, Commercial supercapacitor parameter estimation from step voltage excitation, Int. J. Circ. Theor. Appl. 47 (10) (2019) 1705–1712.
[62] J.E.B. Randles, Kinetics of rapid electrode reactions, Discuss. Faraday Soc. 1 (1947) 11–19.
[63] E.H. Balaguera, J. Bisquert, Accelerating the assessment of hysteresis in perovskite solar cells, ACS Energy Lett. 9 (2) (2024) 478–486.
[64] E. Hernández-Balaguera, B. Romero, B. Arredondo, G. del Pozo, M. Najafi, Y. Galagan, The dominant role of memory-based capacitive hysteretic currents in operation of photovoltaic perovskites, Nano Energy 78 (2020) 105398.